CrossMark

ORIGINAL ARTICLE

Water connectivity in hillslope of upland–riparian zone and the implication for stream nitrate-N export during rain events in an agricultural and forested watershed

Rui Jiang[1,2] · Ryusuke Hatano[2] · Robert Hill[3] · Kanta Kuramochi[2] · Tao Jiang[4] · Ying Zhao[1]

Abstract Water connectivity in the hillslopes of the upland–riparian zone has environmental implications for stream nitrate-N (NO_3^--N) export during rain events. This study was conducted to measure the shallow groundwater table over a hillslope with upland, interface, and riparian forest components and measure the stream NO_3^--N concentrations in a 36.6 km^2 agricultural and forested watershed (AFW) in the Shibetsu area of northern Japan from July to November 2009. The groundwater and stream hydrographs at seasonal and rain event scales indicated that the hillslope water connectivity was first established from the riparian forest, and then expanded to the upland after several rain events. The hillslope water connectivity has important implications for NO_3^--N export in the watershed since the NO_3^--N export may primarily be explained by a flushing mechanism. The NO_3^--N export only flushed from riparian forest during the early water connection stage. While in the well water connection stage, the flush of NO_3^--N occurred with the subsurface flow from the upland which had a high shallow groundwater table and displayed higher stream NO_3^--N concentrations. However, lower stream NO_3^--N concentrations occurred during the late water connection stage and indicated that the N source in the upland might be limited due to denitrification and NO_3^--N leaching processes. Nevertheless, it was decided that the hydrology and biogeochemical reactions occurring in the upland controlled the stream NO_3^--N export. A conceptual model was formulated that explained the impacts of the hillslope water connectivity on the watershed stream NO_3^--N export during rain events in early, well, and late water connection stages within the AFW.

Keywords Shallow groundwater · Hillslope of upland–riparian zone · Water connectivity · Nitrate-N · Conceptual model

Introduction

Previous field studies over the last few decades have documented the hydrological processes on hillslopes and provide a foundation for studies of biogeochemical processes in watersheds (Anderson and Burt 1990; Burt and Pinay 2005; Lexartza-Artzal and Wainwright 2009). An important component of hillslopes is the three-dimensional flow of water which is a critical component in understanding the hydrological and biogeochemical responses within different landscapes in a watershed (Wood 1999). New advances in hillslope hydrology that considers the water connectivity in upland–riparian zones have improved our understanding of the processes and mechanisms involved in runoff generation and nitrate-N (NO_3^--N) transport and export (Ocampo et al. 2006a, b). The water connectivity, or hydrological connectivity, between the

✉ Rui Jiang
  haixia992000@hotmail.com

✉ Ying Zhao
  yzhao@nwsuaf.edu.cn

1 Key Laboratory of Plant Nutrition and the Agri-Environment in Northwest China, Ministry of Agriculture, College of Natural Resources and Environment, Northwest A&F University, 3# Taicheng Road, Yangling 712100, Shaanxi, China

2 Graduate School of Agriculture, Hokkaido University, Sapporo 060-8589, Japan

3 Department of Environmental Science and Technology, University of Maryland, College Park, MD 20742, USA

4 College of Resources and Environment, Southwest University, Chongqing 400716, China

upland zone and the riparian zone occurs via the subsurface flow system, when the groundwater table at the upland–riparian interface is above the confining layer (Vidon and Hill 2004). Some studies have stated the non-linear behavior of the storm response (James and Roulet 2007), various mechanisms of rapid delivery of pre-event water (McGlynn et al. 2002), and different trends for NO_3^--N transport (Ocampo et al. 2006a) that are attributable to differences in hydrological connectivity. These studies have also highlighted the importance of subsurface flow systems and/or a shallow groundwater system for water connectivity in the hillslopes of upland–riparian zones. However, except for complicated situations involving the subsurface flow system or the shallow groundwater system, these systems also depend on some spatio-temporal factors, for example, rainfall and/or snowmelt regimes, unsaturated zone thickness, permeability, and the presence of an impeding layer (e.g., bedrock or clay). Therefore, how these systems influence water connectivity at temporal and/or spatial scales remains a challenge in understanding the water connectivity within the hillslope of the upland–riparian zone.

There are several factors influencing the water connectivity in hillslopes or watersheds, such as the shallow groundwater table, antecedent soil moisture, climate, soil characteristics, and bedrock topography (Ocampo et al. 2006b; Gerritse et al. 1995; Western et al. 2001). Ocampo et al. (2006b) investigated the water connectivity in a Western Australian catchment and stated that the landscape appears to have developed a catenary control through two basic soil units. The large unsaturated zones of permeable upper soils at upland positions enhances the vertical movement of the infiltrating rainwater over the wet period and accumulates within the hillslope at this position until the storage exceeds an apparent threshold before flowing downhill. In contrast, the riparian areas present shallower, higher permeable soils on level to gentle slopes, the increased infiltration of these soils helps to produce a rapid response to rain events. Vidon and Hill (2004) provided a conceptual model of riparian zone hydrology typical of glacial till and outwash landscapes in Ontario, Canada, based on upland storage capacities (i.e., depth of permeable sediment) and topography of the riparian zone. Western et al. (2001) provided experimental evidence of a nonlinear "threshold" response in runoff generation with antecedent moisture conditions influencing and quantifying the patterns of hydrologic connectivity. Shallow groundwater has been found to play an important role in nitrogen losses in hillslopes associated with water connectivity (Gerritse et al. 1995). These previous research studies have addressed the issue that factors control the water connectivity in hillslope or watershed, however, how the water connectivity within hillslope affects streamflow or NO_3^--N

export at the watershed scale is still not clear. Flow paths and the spatial distribution of water in the watershed have a role in determining N export. Water connectivity associated with the hillslope of upland–riparian zones may provide a complete route for NO_3^--N transport from upland to stream, thus representing the stream NO_3^--N export. However, some studies have shown that during baseflow conditions, the relationships between water sources and N export could be altered by processes occurring in the upland–riparian zones such as denitrification due to water connectivity in these areas (Hill 1996; Hill et al. 1999; Schade et al. 2005; Ocampo et al. 2006a, b). Obviously, there are still many unknowns concerning the contributions of water connectivity to N export related to hydrological and biogeochemical processes occurring at hillslope and watershed scales.

NO_3^--N export mechanisms have been explained by (1) a flushing mechanism (Creed et al. 1996), where NO_3^--N that accumulates in upper soil layers is flushed with subsurface flow to the stream by a rising groundwater table during storms; (2) a draining mechanism (Creed and Band 1998a), where NO_3^--N rich snowmelt water recharges deep groundwater via preferential flow paths and is released during storms and baseflow; and (3) combined flushing and draining mechanisms (McHale et al. 2002). In the Shibetsu watershed, a previous study has stated that the NO_3^--N export can be mainly explained by the flushing mechanism during rain events (Jiang et al. 2010). Therefore, the water connectivity in the hillslope that is related to the subsurface flow system or the groundwater system may regulate the NO_3^--N export in the watershed since the NO_3^--N export may be dominated by a flushing mechanism. Ocampo et al. (2006b) studied the hydrological connectivity of upland–riparian zones in an agricultural watershed, and found that a shallow groundwater system became established all the way across the hillslope. The groundwater system provided a direct hydrological connection between the two zones, and enabled not only the downslope transport of fresh water, but also nitrates that had previously accumulated in the upland zone. Creed and Band (1998b) hypothesized that variation in the export of NO_3^--N is tightly linked to variations in the variable source area (VSA) dynamics among the catchments and represents the intersection of the saturated wedge with N near or at the soil surface. The VSA is related to the shallow groundwater system and may also be regulated by the water connectivity in the hillslope. In order to test the relationships between water connectivity and NO_3^--N flushing mechanism, the agricultural and forested watershed (AFW) located in the center of Shibetsu watershed was chosen in this study. The present study focused on the shallow groundwater in the hillslope of upland–riparian zone and stream NO_3^--N export, to (1) investigate the

hillslope water connectivity at seasonal and rain event scales in the agricultural and forestry watershed; and (2) establish a conceptual model linking the hillslope water connectivity to stream NO_3^--N export at the watershed scale.

Materials and methods

Site description

The 36.6 km^2 agricultural and forested watershed (AFW) is a sub-watershed of the larger Shibetsu watershed (Fig. 1), located in the east of Hokkaido, Japan. The land use is primarily composed of agriculture (58.9 %) and forest (37.1 %) with over 95 % of the agriculture land being used for grassland or pasture. Upstream areas with steep slopes (>10°) are covered by forest and middle/lower stream areas are generally agricultural land with gentle slopes (<5 %). Soils consist of Regosolic kuroboku soils (50.9 %), Brown lowland soils (22.7 %), Kuroboku soils (18.9 %), and Brown forest soils (7.5 %). Agricultural soils are predominately Regosolic kuroboku soils and Kuroboku soils, both of which are about 1 m in depth. Major vegetation types are *Phleum pratense* (grassland/pasture) and Japanese larch—*Larix kaempferi* (forest). Fertilization in the grassland/pasture areas was conducted during spring and summer using chemical fertilizer at a rate of 66 kg N ha^{-1} $year^{-1}$ and during summer and autumn using manure to supply a N rate of 193 kg N ha^{-1} $year^{-1}$ (manure data

were calculated from information provided by the Agricultural Department of Hokkaido Government (2002–2009). In the Shibetsu area, the mean annual temperature is 5 °C and the mean annual precipitation is 1158 mm. The snow period persists from early December to late April with a mean value of 484 cm for annual snowfall. Stream discharge varies with seasons at the outlets of headwater streams and the Shibetsu watershed. Peak stream discharge occurs during the snowmelt season and again in August to November during rainfall events (1981–2010, Japan Meteorological Agency 2011, http://www.jma.go.jp/jma/indexe.html). The selected hillslopes of the upland–riparian zones are located in the downstream areas (Fig. 1) with flat slopes ranging from 0.9–2.3 % and hillslope lengths of about 50 m. The upland areas are utilized for grassland/pasture and the riparian zones are under forest vegetation. The vegetation in the riparian forests is dominated by broadleaf trees such as Hokkaido willow (*Salix rorida* Lackschewitz), alder (*Alnus japonica* Steud.), and magnolia (*Magnolia obovata* Thunb.).

Watershed sampling

Stream water samples were collected using autosamplers installed at the outlet of the AFW during three rain events in 2009: July 18 (E1), October 8 (E2), and November 14 (E3). The autosampler was triggered when rainfall was >4 mm per 30 min^{-1} with intervals of 15 min to 1 h for the rising stage of discharge and from 2 to 6 h for the receding stage. Stream discharge rates at baseflow were

Fig. 1 Map of the agricultural and forested watershed (AFW) shown as a sub-watershed of the larger Shibetsu watershed located in the east of Hokkaido, Japan, and the location of the hillslope of upland–riparian zone within the AFW watershed
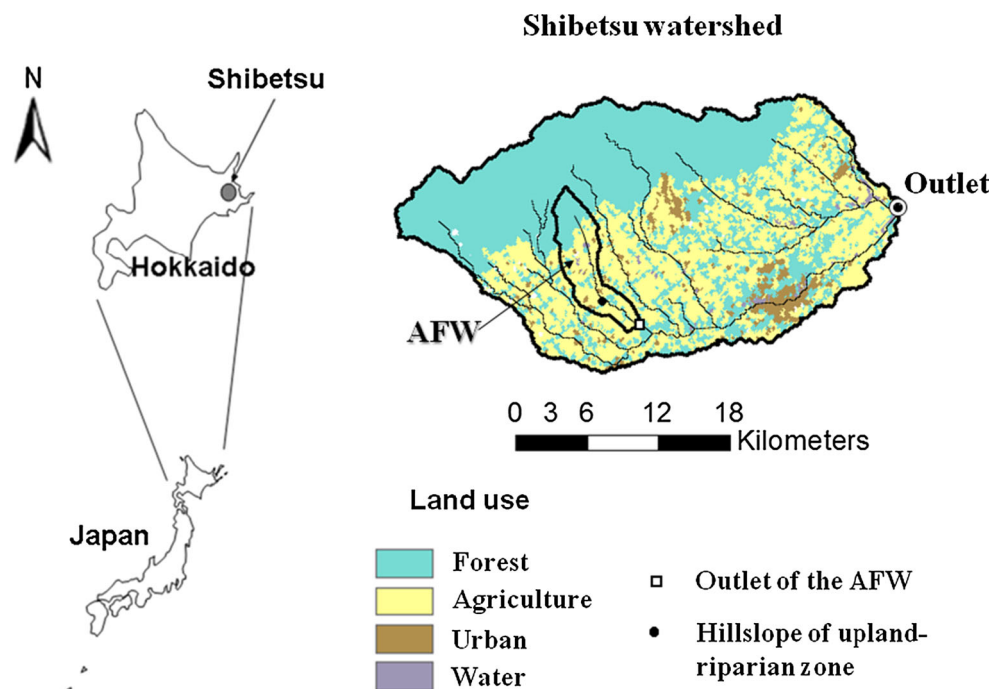
measured using a flow velocity meter (TK-105; Toho Dentan, Tokyo) at the outlets of the watersheds. The discharge rates were calculated by multiplying the sectional area of the stream by the flow velocity measured along a transect across the stream. The stream water table was recorded every 15 min by water sensors equipped with data loggers (MC-1100 W, STS, Sirnach, Switzerland) installed in stream near autosamplers. Stream discharge was calculated from the stream water table using calibrated H-Q equations (i.e., quadratic curve) modeling the relationships between discharge (Q) and water table (H) (Tachibana and Nasu 2003). Meteorological data were obtained from the Japan Meteorological Agency (http://www.jma.go.jp/ima/indexe.html).

Upland–riparian zones instrumentation

A total of three transects perpendicular to the streamflow were composed of 15 shallow groundwater wells that were installed at hillslope positions across the upland, at the interface of the upland and the riparian zones, and within the riparian zones (Fig. 2). The shallow wells consisted of 5 cm diameter PVC pipe that was screened along the entire depth of the well. The shallow wells were installed at soil depths, up to 2 m, according to the location of a clay layer that was determined using hand augers. Shallow groundwater levels were measured monthly from July to November, 2009. Pressure sensors and water loggers were set up for shallow wells B1, B2, B3, and B5 in the middle

transect to record the groundwater table at 15 min intervals from early July, 2009. Wells B1, B2, B3, and B5 represent wells placed in upland, interface, riparian zone, and riparian edge landscape positions, respectively. Lysimeters were installed next to the groundwater wells at a 50 cm depth of the soil profile position. Three lysimeters were located in the upland, and two lysimeters were located in the middle of the riparian forest. These lysimeters were sampled monthly.

Chemical analysis

The water samples were analyzed for total N (TN) by the method of alkaline persulfate digestion using HCl-acidified UV detection. After filtering through 0.2 μm membrane filters, water samples were analyzed for total dissolved N (TDN), NO_3^--N, NH_4^+-N, Si, and dissolved organic carbon (DOC). The TDN was determined by the same method as TN. The NO_3^--N was determined by ion chromatography (QIC Analyzer; Dionex, Sunnyvale, CA); NH_4^+-N was determined by colorimetry using the indophenol blue method; and Si was determined colorimetrically by the molybdenum blue method. The DOC was determined by a total organic carbon analyzer (TOC-5000A, Shimadzu, Japan).

Soil samples were collected monthly in the areas of the upland, the interface, the riparian zone, and the riparian edge. All the soil samples were air dried and ground to pass a 2 mm sieve for NO_3^--N, TN, NH_4^+, denitrification

Fig. 2 Topographic map of the studied hillslope area composed of upland–riparian zones within the agricultural and forestry watershed. Specific information includes the elevation contour lines showing the grassland, interface, and riparian forest land use zones; location of the A, B, and C transects; and placement of shallow wells
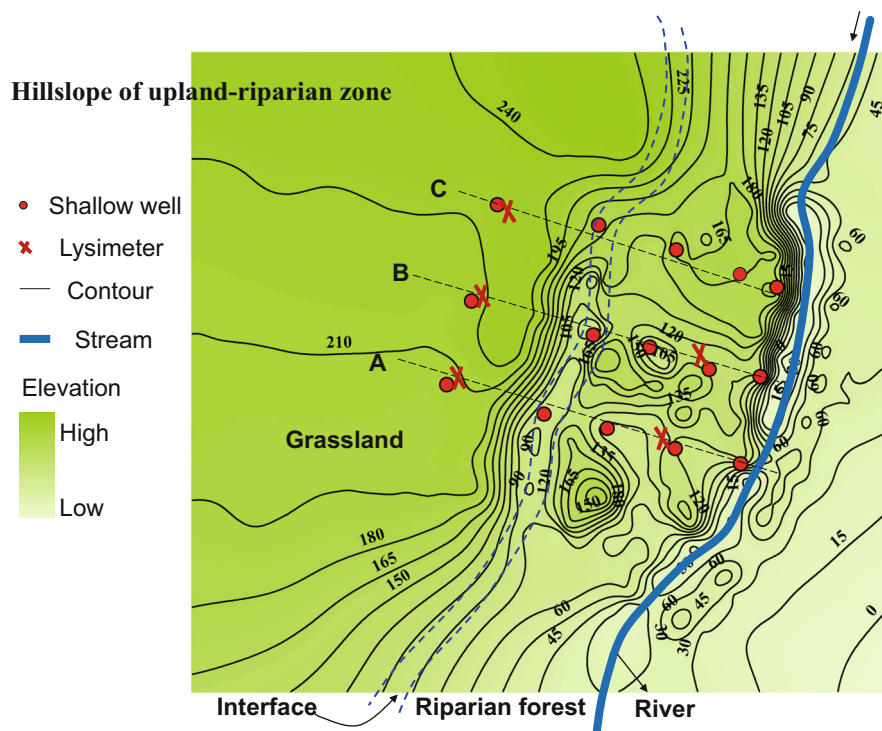
potential, net mineralization rate, and nitrification rate analysis. NO_3^--N and NH_4^+ in the soil were extracted using a 1:5 soil:2 M KCl solution and the concentrations were determined by colorimetry as a water sample. Denitrification potential was determined using the acetylene block technique, which inhibits the final conversion of N_2O to N_2 gas (Tiedje 1994). To determine the differences among the sites in the amount of organic C available to denitrifying organisms, we defined denitrification potential as the denitrification rate that occurred under anaerobic conditions with abundant NO_3-N at 25 °C. Samples of fresh, homogenized soil (15 g) were placed into 100 mL serum bottles. An aliquot of 15 mL solution treated with NO_3-N (200 mg N L^{-1} as KNO_3) and chloramphenicol (2 mg L^{-1}) was added to the bottles. The serum bottles were evacuated and flushed four times with N_2 to ensure anaerobic conditions, and acetylene (C_2H_2) gas was added to a final concentration of 10 % (10 kPa) in the headspace. Headspace gas was sampled by syringe at 2 and 4 h and denitrification rates were calculated from the linear portion of N_2O produced over time. Nitrous oxide was determined using a gas chromatograph with an electron capture detector (GC-14B; Shimadzu). A 50 g dry soil was put into a 100 mL beaker and added 20 mg of aqueous $(NH_4)_2SO_4$ to maintain the water content at 40 % of the field capacity. Then the beaker was covered by aluminum foil and incubated at 27 °C for 30 days in the dark. At the end of the incubation, the nitrate-N was extracted with 100 mL H_2O and the ammonia-N was extracted with 2 M KCl solution and then determined by colorimetry. Changes in inorganic N content in the control treatment during a 30 day period represented net nitrogen mineralization. The increase in the nitrate-N during the course of the laboratory incubation is referred to as the net nitrification. Net N-mineralization rates were thus estimated as the net increases in ammonium-N plus nitrate-N, and the net nitrification rates were calculated as the net increase in nitrate-N that occurred during the first 30 days of the incubation.

Results and discussion

Seasonal stream water and hillslope shallow groundwater hydrographs

The annual precipitation was 1606.5 mm in 2009, which was 40 % greater than the mean annual precipitation. From July to November, the total rainfall amount was 847.5 mm. Precipitation in July, September, and October contributed large portions of the rainfall during our studied period and accounted for 35, 20, and 22 % of the total annual precipitation, respectively. Rain events that occurred in August and November were minimal and accounted for only

14 and 9 % of the total annual precipitation, respectively. Stream water tables showed a series of peaks and well water levels generally responded to the precipitation events (Fig. 3). In early July, the stream water table was low, but increased sharply during a 31 mm rain event in the middle of July, and then increased again during an 81 mm rain event on 25 July. The stream water table maintained a high level from the end of July to the middle of October and then decreased gradually during November because of less rain.

Shallow groundwater table dynamics showed clear differences in response to the rain events, depending on the position along the hillslope (Fig. 4). Water tables in wells located within the riparian forest edge (B5) responded rapidly as did the stream water table over the same time scale of rain events, although some portion of the data was lost due to a broken logger. The B3 well located in a hollow in the riparian forest with a 0.75 m unsaturated zone thickness also increased the well water level in response to the rain events, but there were no obvious increases or decreases in the well water levels at the seasonal scale. Well B2 located at the interface of the upland and the riparian forest responded differently during rain events. Water table fluctuations occurred within an unsaturated zone of up to 1.8 m and the water well levels responded to rain events from July to September. There was a slight increase after an 81 mm rain on 25 June, but a large increase was shown after a 63 mm rain event on October 2nd. When the second rain event in October occurred, B2 showed the largest peak during our studied period and then maintained a high level (12 cm higher than that during July to September, on average) till the end of October. In November, the water level was still high, but 4 cm (on average) lower than the levels observed in October. The response of B1 located in the upland with an unsaturated
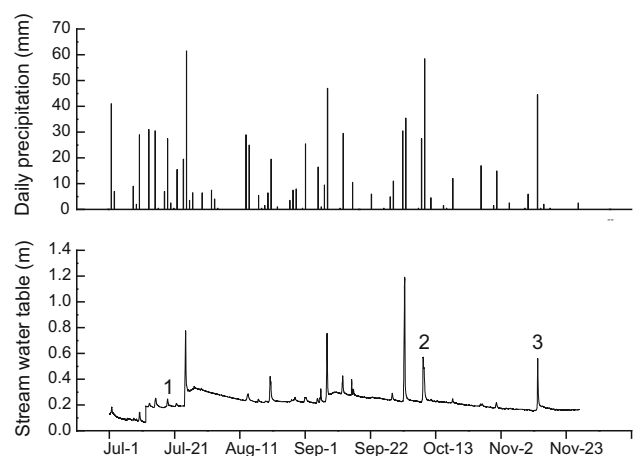
Fig. 3 Response of stream water table to precipitation (the *number* in the *graph* refers to rain events sampled)

Fig. 4 Time series of water table (depth below surface) at 15 min interval in stream and the shallow perched aquifer from July to November. *B1* is in upland, *B2* is located at the interface of upland and riparian zones, *B3* is at the hollow in riparian zones, *B5* is in riparian edge close to stream
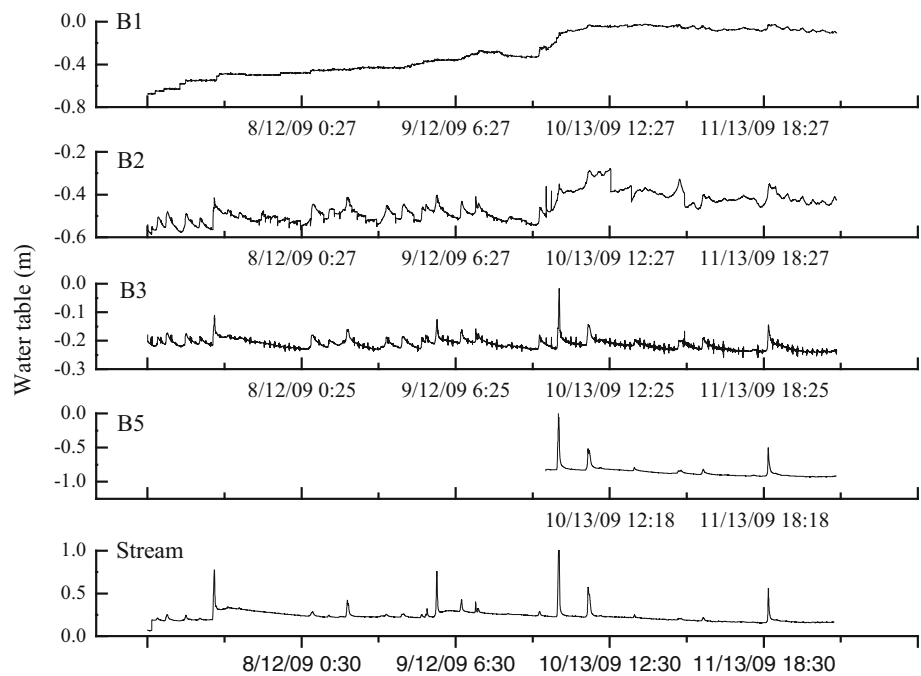
zone over 2 m in thickness responded differently than the other wells. Well B1 did not show an immediate response to rain events, but increased gradually from July to the end of September. A sharp increase of approximately 20 cm occurred in the water table after two rain events in early October in which the water table reached the top soil layer within 5 cm of the soil surface. Well B1 also showed several small peaks during the rain events in October and November. These data suggested that the groundwater tables at the upland displayed a smoother response record that reflected the seasonal variability of the rain events and a delayed response due to shallow storage effects. At the same time, the interface displayed a water level response that was somewhat intermediate to the responses displayed by the upland and riparian zones.

We measured the groundwater table of all three transects manually during baseflow from July to November, so the seasonal changes in the groundwater table in the upland–riparian zones might be more clearly visualized by looking at the groundwater tables on the three cross sections of the hillslopes (Fig. 5). The groundwater tables in the shallow aquifer were very low in early July. After the occurrence of a series of rain events, the upland and the interface shallow aquifer recharged considerably in late September and maintained or slightly increased the levels in October/November. However, the groundwater tables in the riparian zones didn't display much seasonal change. In addition, the groundwater table of upland wells located on steep hillslopes (A1 and B1) increased much more in September than the groundwater table located on the flat hillslopes

(C1). A1 displayed its highest water table in November, which was later than B1 and C1, and implied that soils on the flatter landscape positions were easier to saturate.

Rainfall hydrographs and water connectivity at upland–riparian hillslope during rain events

The three rain events were characterized by different hydrological characteristics (Table 1). Rain event E1 had the smallest quantity of rainfall, but displayed the largest values for the antecedent precedent precipitation index (API_7 and API_{21}). Rain event E2 displayed the highest mean discharge rate with the largest total precipitation and second highest rain intensity. The runoff coefficient increased from E1 to E3, which indicated that the watershed was getting wetter and the water storage in the shallow aquifer was increasing. There was an inverse relationship displayed for the API_x and the runoff coefficient for rain events E1 and E3. Event E1 resulted in a higher API_x but lower runoff coefficient value, while event E3 displayed a lower API_x, but higher runoff coefficient. These differences were likely due to higher rates of evapotranspiration and the larger water use for vegetation combined with a lower water table in the shallow aquifer in July, and lower rates of evapotranspiration and lower water use combined with a higher water table in November.

The groundwater table follows a different pattern for E1 (upland well B1 < interface well B2 < riparian well B3) versus E2 and E3 (riparian well B5 < interface well B2 < riparian well B3 < upland well B1) (Fig. 6). During
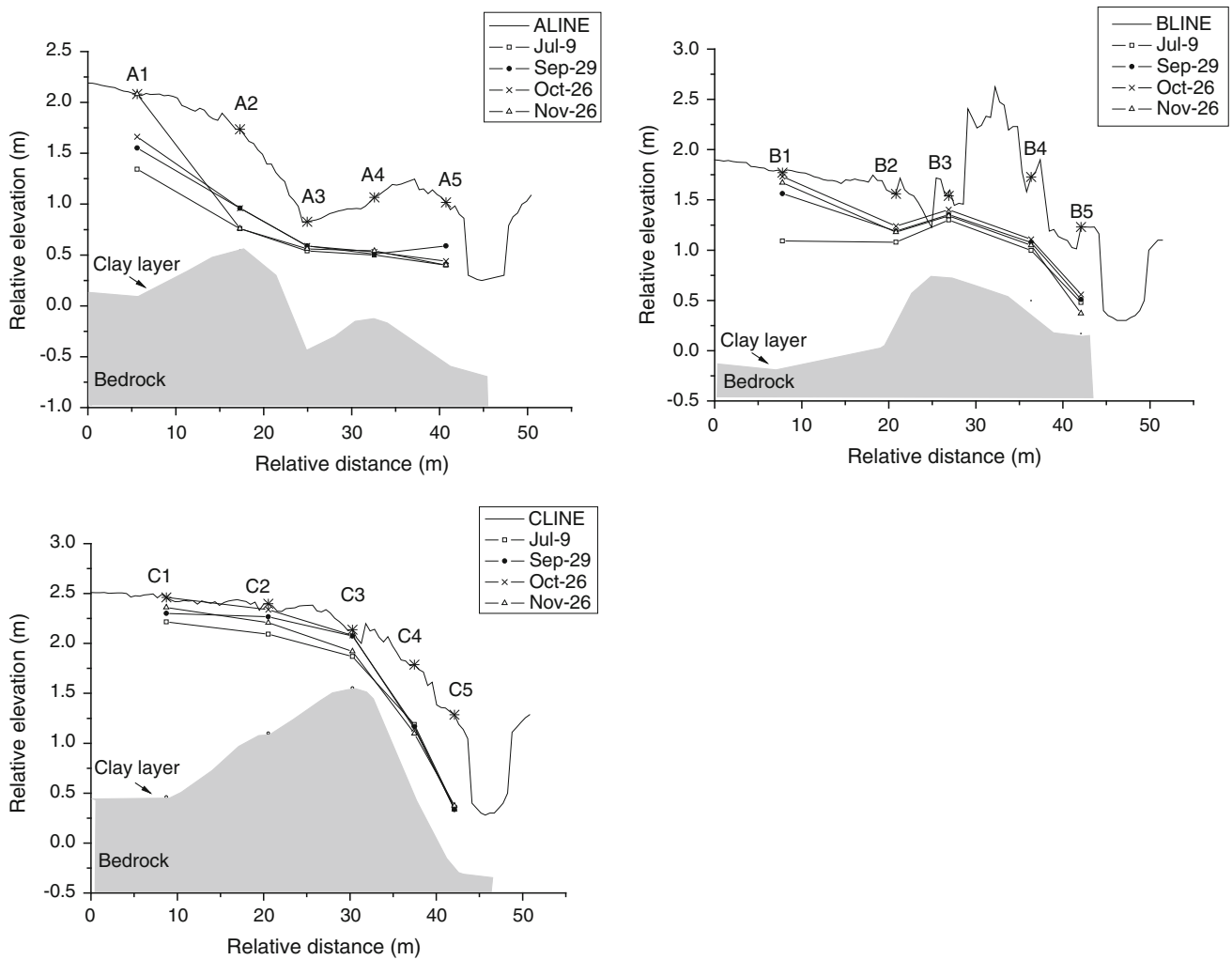
Fig. 5 Temporal evolution of water table in the shallow aquifer across the hillslope from July to November (three transects: A, B, and C). *A1*, *B1*, and *C1* are in upland; *A2*, *B2*, and *C2* are located at the interface of upland and riparian zones; *A3*, *B3*, and *C3* are at the hollow in riparian zones; *A4*, *B4*, *C4*, *A5*, *B5*, and *C5* are in riparian edge close to stream

Table 1 Hydrological characteristic of rain events, the antecedent precipitation index (API$_x$), mean stream discharge, and runoff coefficient for the agricultural and forested watershed (AFW)

| Rain event	Date	Precipitation		Rainfall duration (h)	API$_x$[a]		Mean discharge (m^3 s^{-1})	Runoff coefficient[b]
		Total (mm)	Max (mm/h)		API$_7$	API$_{21}$		
E1	7/18–20	37	5.0	22	16.6	24.3	0.98	0.18
E2	10/8–10	86	7.5	24	12.7	14.8	1.96	0.19
E3	11/14–16	44.5	9.0	18	2.1	4.6	1.26	0.21

[a] API$_x$ antecedent precipitation index, presents the pre-event soil moisture of the watershed. The API for x preceding days is defined as follows: $API_x = \sum_{i=1}^{x} \frac{p_i}{i}$

where $x = 7$ or 21 days before a rainfall event and P_i (mm) is the total precipitation on the ith day before the event (Jiang et al. 2012)

[b] Runoff coefficient is defined as mean stream discharge divided by total volume of precipitation

rainfall events E2 and E3, the groundwater table in the riparian edge well B5 was the first groundwater well to peak in response to the high intensity rainfall and then quickly dropped to pre-event levels (Fig. 6b, c). The stream water peak was slightly later than the B5 peak, but was maintained for a longer time before returning to pre-event
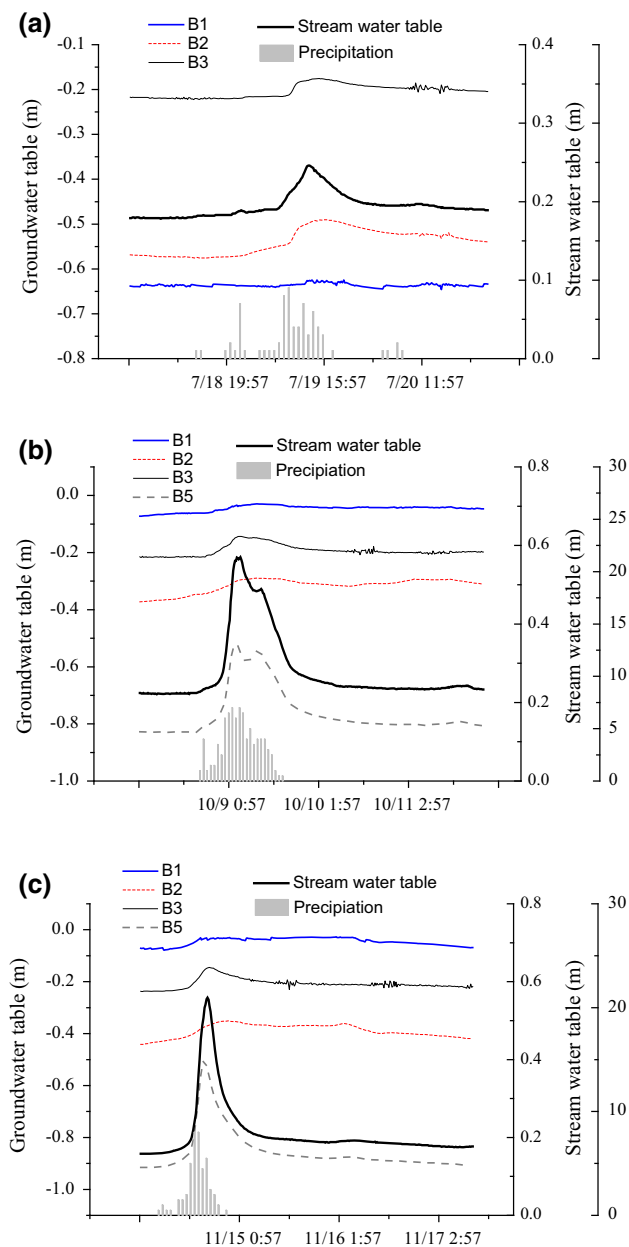
Fig. 6 Precipitation depth, stream water depth, and ground water table depth for time periods immediately before, during, and after rain events occurring on **a** July 18 (*E1*), **b** October 8 (*E2*) and **c** November 14 (*E3*), 2009. *B1* is in upland, *B2* is located at the interface of upland and riparian zones, *B3* is at the hollow in riparian zones, *B5* is in riparian edge close to stream. There is no data for *B5* in *E1* due to the broken data logger

levels. Riparian zone well B3 and interface well B2 both displayed peaks in response to the events, but the peaks were diminished in comparison to the response of well B5. Wells B3 and B2 had relatively equivalent peak responses to event E1, but well B3 displayed slightly higher peaks than B2 in response to events E2 and E3. The groundwater table in B3 was at about a −20-cm depth at the initiation of all rain events. Interface well B2 had groundwater tables at

about −55, −30, and −40 cm at the initiation of events E1, E2, and E3, respectively.

Upland well (B1) was relatively stable during rain events and only displayed a very small if any increase after event E1 and small responses after events E2 and E3 (Fig. 6). The groundwater in B1 peaked quickly with peak discharge only during events E2 and E3, however, the groundwater peak patterns in B2 and B3 occurred during all the three events. It also should be noted that the groundwater table for B1 was at approximately a −65-cm depth during event E1 and was near the surface during events E2 and E3. These phenomena suggested that the pattern displayed in wells were likely associated with the antecedent groundwater table or the shallow groundwater storage.

The seasonal and rain event variations of streamflow and shallow groundwater tables at upland, interface, riparian forest hollow, and riparian forest edge showed where and when the water connections occurred (Figs. 4, 5, 6). The data indicated that there was low streamflow in response to the low groundwater table in early July, a rapid rising limb for streamflow associated with a quick response of the riparian forest groundwater to rain events, and no response for the upland groundwater in middle July. These observations showed that the water connectivity was developed, but was only well connected within the riparian zones during middle July. We defined this period as early water connection stage and the rain event E1 belongs to this stage. A large increase of groundwater table in interface wells and upland wells in October and November indicated the strength of increased connections and the development of full connectivity from the upland to the stream which was defined as the well connection stage. Though the groundwater tables in the upland and the interface were still high in November, the slight decreases for both stream water table and groundwater table suggested that the connections from the upland to the stream would be lost gradually due to less rainfall, thus we named it as the late connection stage. The rain events E2 and E3 occurred during the well and late connection stages, respectively.

Stream water NO$_3^-$-N export during rain events

NO$_3^-$-N concentrations showed a fluctuating, but decreasing trend with an average value of 1.22 mg L^{-1} from the beginning to the end of event E1 (Fig. 7). During E2, NO$_3^-$-N sharply peaked and then decreased before the stream discharge peak occurred. The peak concentration was up to 2 mg L^{-1} and the average value was 1.59 mg L^{-1}. Although NO$_3^-$-N concentrations during event E3 also displayed a peak concentration, the concentrations initially decreased during peak discharge and then displayed a fluctuated trend that increased until a peak

Fig. 7 Stream discharge and stream concentrations of nitrate nitrogen (NO_3^--N), dissolved organic carbon (DOC), and silicon (Si) shown for time periods immediately before, during, and after rain events occurring on July 18 (*E1*), October 8 (*E2*), and November 14 (*E3*), 2009
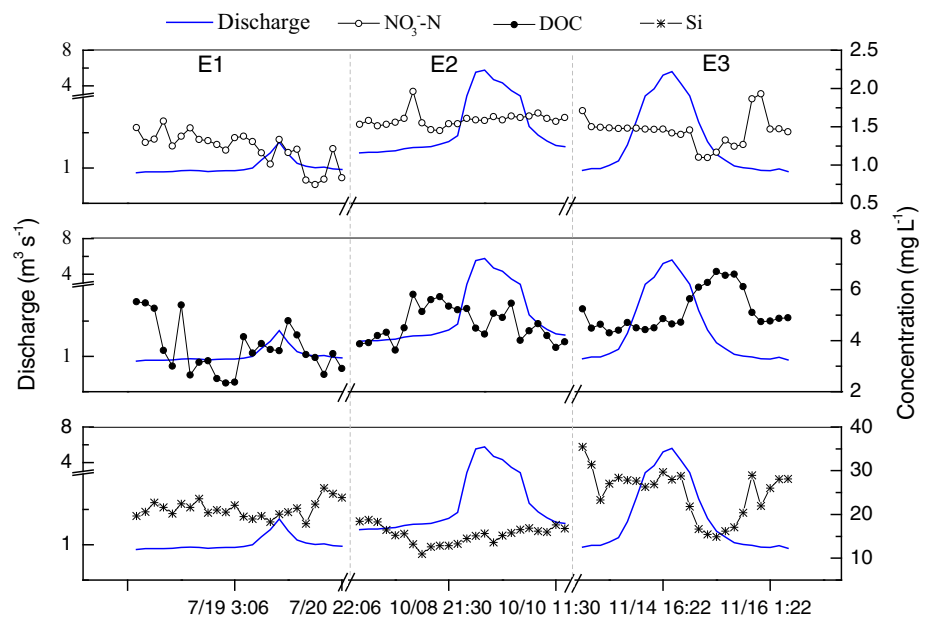
concentration was displayed after peak discharge. The average NO_3^--N concentration of E3 was 1.44 mg L^{-1} with a maximum value of 1.93 mg L^{-1}.

We used DOC and Si as indicators to examine the water and nitrate sources, because DOC represents the solute that typically accumulates water in surficial soil layers and is exported with subsurface runoff. High Si concentrations have typically been associated with deep groundwater and/or water with a high residence time in the watershed (Inamdar and Mitchell 2006). The results showed that the DOC had two main peaks in E1 (Fig. 7). One sharp and short increase occurred before discharge peaked, while the second increase occurred with the discharge peak. In E2, the DOC increased before the discharge peaked and decreased as the discharge peak decreased. By contrast, the DOC peaked after the discharge peak in E3. The DOC peaks occurred at different times during rain events and implied that the subsurface runoff displayed different responses to each rain event. Si also displayed different trends during the three rain events (Fig. 7). Si fluctuated with small waves and was comparatively stable during E1. An opposite trend of Si to discharge behavior was shown in E2 as the Si decreased when the discharge peaked. A revised trend also existed between the Si and the DOC in E3 as the DOC peaked after the discharge peak and the Si concentration decreased to a minimum as the peak discharge was decreasing. However, the Si concentrations had the same trends with the NO_3^--N concentrations in E3 which first displayed a decrease and then a peak concentration after the peak discharge.

Soil and water chemistry of upland–riparian zone

Table 2 indicates that the surface soil TN and NH_4^+-N were lower in the near-stream zones (riparian edges); while the NO_3^--N concentrations were much higher in the upland and the near-stream zones than in the riparian zones. Riparian zones had high water contents, low mineralization rates, low nitrification rates, high denitrification rates, and low NO_3^--N concentrations. In contrast, the upland and the near-stream zones had low water contents, high mineralization rates, high nitrification rates, low denitrification rates, and high NO_3^--N concentrations. The inverse trends implied that the NO_3^--N accumulated in the surface soil during the baseflow periods and was related to the soil moisture and biogeochemical processes (i.e., mineralization, nitrification, and denitrification).

The monthly mean NO_3^--N concentrations in the upland soil water were much higher than the concentrations in the riparian soil water and the spring water (Table 3). The NO_3^--N concentrations tended to decrease from July to November in the upland soil which indicated that the NO_3^--N source may be limited. However, the NO_3^--N concentrations in the riparian soil water first increased and then decreased and may be related to the NO_3^--N source from the upland soil. The NO_3^--N concentrations in the spring water were quite stable. The NH_4^+-N concentrations in the upland soil water also decreased and suggested that N transformations were occurring. The Si concentrations in the upland soil water and the riparian soil water were much lower than the concentrations in the spring water. The DOC concentrations in the upland soil water increased from July

Table 2 Mean concentrations of surface soil chemistries in upland–riparian zones according to monthly measurement during July to November

Point	NH_4^+-N (mg N kg dry soil^{-1})	NO_3^--N (mg N kg dry soil^{-1})	TN (%)	Water content (%, dry soil base)	Mineralization rate (mg N kg dry soil^{-1} day^{-1})	Nitrification rate (mg N kg dry soil^{-1} day^{-1})	Denitrification rate (mg N kg dry soil^{-1} day^{-1})
Upland	4.46 (0.77)	45.11 (9.18)	0.20 0.01	55.03 (2.29)	1.53 (0.28)	0.91 (0.43)	133.13 (91.49)
Interface	5.11 (3.66)	17.21 (10.39)	0.19 0.04	69.66 (12.89)	1.21 (0.08)	0.58 (0.52)	454.86 (599.24)
Riparian	5.41 (1.37)	10.75 (10.25)	0.20 0.08	101.60 (12.47)	1.11 (0.72)	0.60 (0.32)	659.51 (316.54)
Riparian edge	3.18 (0.77)	52.71 (16.17)	0.13 0.06	47.31 (11.44)	1.53 (0.47)	1.22 (0.53)	118.19 (43.37)

Standard error is in parentheses

Table 3 Mean concentrations of water chemistries in various sources according to monthly measurement during July to November

	July	September	October	November
NO_3^--N (mg L^{-1}) in upland soil water	9.26 (2.40)	7.18 (3.54)	8.67 (1.00)	3.46 (1.43)
NO_3^--N (mg L^{-1}) in riparian soil water	1.22 (0.79)	3.34 (1.20)	2.35 (0.46)	1.38 (0.74)
NO_3^--N (mg L^{-1}) in spring water	3.89 (0.72)	3.96 (0.56)	4.29 (0.49)	4.34 (0.80)
NH_4^+-N (mg L^{-1}) in upland soil water	2.86 (3.93)	1.51 (1.35)	0.16 (0.22)	0.36 (0.21)
NH_4^+-N (mg L^{-1}) in riparian soil water	0.11 (0.05)	0.11 (0.12)	0.02 (0.03)	0.02 (0.00)
NH_4^+-N (mg L^{-1}) in spring water	0.17 (0.03)	0.15 (0.06)	0.05 (0.02)	0.04 (0.01)
Si (mg L^{-1}) in upland soil water	4.23 (1.56)	3.68 (1.20)	1.65 (0.40)	2.2 (1.28)
Si (mg L^{-1}) in riparian soil water	6.01 (1.01)	8.00 (2.47)	10.27 (0.91)	6.50 (4.79)
Si (mg L^{-1}) in spring water	39.43 (0.51)	40.21 (0.83)	39.13 (0.35)	40.63 (0.78)
DOC (mg L^{-1}) in upland soil water	5.74 (1.68)	11.80 (3.47)	10.12 (1.66)	17.22 (6.81)
DOC (mg L^{-1}) in riparian soil water	5.39 (2.20)	9.38 (1.05)	5.71 (4.67)	9.55 (0.54)
DOC (mg L^{-1}) in spring water	–	–	–	–

Standard error is in parentheses

to November and are attributed to the litter decomposition during autumn.

The implications of hillslope water connectivity for stream NO_3^--N export

The observed stream NO_3^--N export showed similar trends with the DOC concentrations in wells E1 and E2, but an opposite trend with the DOC concentrations, and the same trend with Si concentrations was observed for well E3 (Fig. 7). These results suggested that the shallow and deep groundwater both may contribute to the stream NO_3^--N export in the AFW. During rain events, the NO_3^--N export was likely explained by the upland groundwater contributions in the Shibetsu watershed using a flushing mechanism (Jiang et al. 2010). Jiang et al. (2010) described that the accumulated NO_3^--N in the upper soil layers was flushed to the stream by a rising groundwater table during storms. However, the upland groundwater in the AFW was fundamentally controlled by the water connectivity of the upland–riparian zones and is, therefore, related to the hydrologic connectivity, antecedent soil moisture, and the groundwater table (Ocampo et al. 2006b; Jiang et al. 2010). During the E1 event, the depth of the shallow groundwater

table in the upland soil was low (e.g., B1 in Fig. 6a). The large unsaturated zones of high hydraulic conductivity in the upland soil enhanced the vertical movement of infiltrating rainwater during the rain events, and resulted in the formation of a shallow aquifer until the storage exceeded an apparent threshold and started flowing downhill. In contrast, the depth of groundwater table in the riparian zones was much higher (Fig. 6). The riparian zones presented a lower landscape position with highly permeable soils on a level to gentle slopes which facilitated internal drainage, but were limited in their water storage capacity, thus leading to a quick response from rain events (Ocampo et al. 2006b). Hence, the water connectivity was first built within the riparian zones and the riparian groundwater was first flushed during the E1 event. The NO_3^--N accumulated in the riparian zone edges and because of the high nitrification/mineralization and the low denitrification potential (Table 2) became a contributing source of NO_3^--N (Ohrui and Mitchell 1998). Therefore, the excessive NO_3^--N was flushed with the flushing of the shallow groundwater in the riparian zones (Fig. 8a). The NO_3^--N export during the discharge peak coincided with the shallow groundwater peak and the decreased Si concentrations (Fig. 7), which supported the hypothesis that the flushing mechanism had

occurred in the riparian zones. The high NO_3^--N concentrations in the upland soil water, but low concentrations in the riparian soil water during July (Table 3) may also serve as evidence to show that the water connection was only built within the riparian zones. However, the quantities of NO_3^--N in the riparian zones was limited (Table 3) due to the high denitrification potential (Table 2; Hayakawa et al. 2012), thus, we observed that the NO_3^--N peaked with the riparian groundwater peak, but the relative concentrations were not high. The NO_3^--N data for the E2 and E3 events both showed that the NO_3^--N concentrations quickly peaked before the discharge peaks (Fig. 7) and indicated that the deep groundwater acted as the primary source of the stream water and the exported NO_3^--N. We also observed high NO_3^--N concentrations (Table 3) in the

springs within this area. The spring water with high Si concentrations (Table 3) is regarded as deep groundwater. The deep groundwater in this area usually has such high Si concentrations, because most underlying rocks in this area are volcanic ash and the Si is derived from the weathering of that ash (Shoji et al. 1993). Therefore, the combined flushing and draining mechanisms which were mentioned by McHale et al. (2002) seemed to help explain the results of our study.

When the water connectivity was well established, the concentration trends of Si and DOC (Fig. 7) indicated that the upland shallow groundwater increased sharply during the E2 and E3 events and were both characterized by high groundwater tables (Fig. 6). However, the upland groundwater peaked before the discharge peak during the E2 event and after the discharge peak during the E3 event. This difference in the groundwater dynamics is most likely attributed to the differences in the antecedent soil moisture (i.e., the API_x values in Table 1). Although the upland groundwater might have been a major water source during the E2 and E3 events, there was a NO_3^--N concentration peak that coincided with the peak of the upland groundwater during the E2 event. There was also a decrease in the NO_3^--N concentrations observed during the peak of the upland groundwater level during the E3 event. The antecedent soil moisture might have affected the pattern of the NO_3^--N flushing (McNamara et al. 2008; Jiang et al. 2010); while the fluctuation of the groundwater table depth could have some influence on the variable source area (VSA) dynamics as proposed by Creed and Band (1998b).

The high NO_3^--N export with large amounts of the upland groundwater during the E2 event suggested that the NO_3^--N flushed with the largest source area not only from the riparian zones, but also from the upland areas (Fig. 8b). The high NO_3^--N concentrations in upland soil and water soil (Tables 2, 3) also implied that the NO_3^--N was originated from the upland near-surface soil. Our previous studies demonstrated that the stream NO_3^--N concentrations were positively correlated with the NO_3^--N contributions from the upland areas (Hayakawa et al. 2006; Woli et al. 2004). The source of the high NO_3^--N concentrations accumulated in near-surface soil were attributable to the high N fertilizer and/or manure application in the uplands of this area (Jiang et al. 2010) and would be the largest NO_3^--N source during the rain events that occurred in the well water connection stages. However, the low NO_3^--N concentrations in the upland groundwater during the E3 event (Fig. 7) might support the idea of a limited NO_3^--N source as described by Creed and Band (1998b). During the rainy season, the upland–riparian zones may be well connected such that the groundwater table would be sustained near the surface soil layer and would result in soil moisture conditions that would likely enhance the denitrification
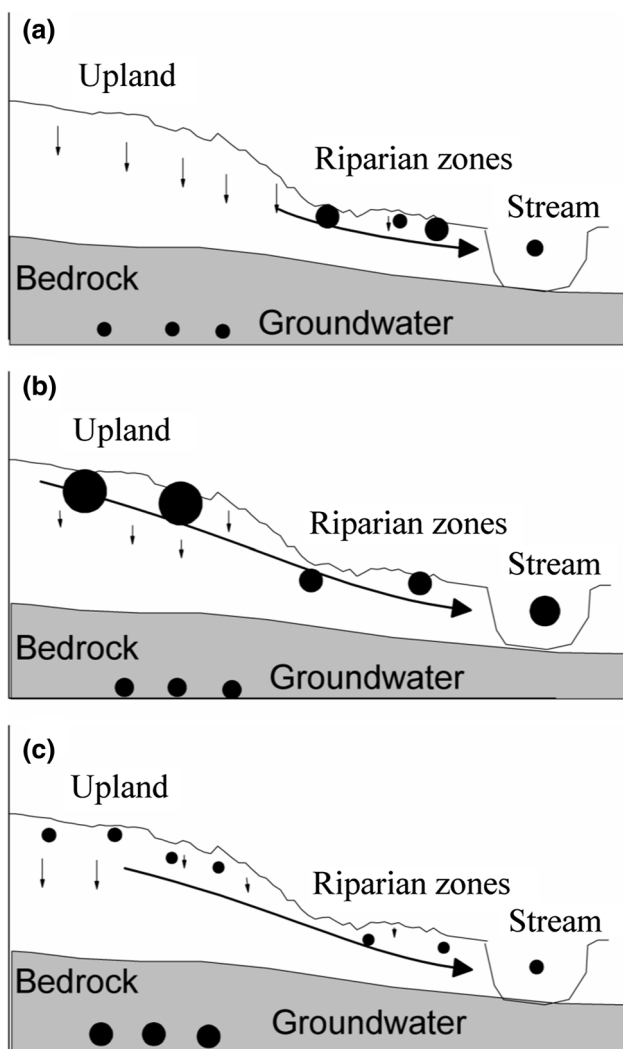
Fig. 8 Conceptual model illustrating nitrate nitrogen (NO_3^--N) export in the agricultural and forested watershed for time periods during early (**a**), well (**b**), and late (**c**) water connection stage. *Circles* indicate NO_3^--N concentrations and *arrows* indicate the means of water connection and the groundwater table depth

process in the upper surface soil layer. The biogeochemical processes of denitrification in association with the leaching in response to the multiple rain events may reduce the soil NO_3^--N to the observed levels. The NO_3^--N concentrations in the upland soil water had lower NO_3^--N concentrations during the late water connection stage (Table 3). Thus the low NO_3^--N export with the increase of the upland groundwater may be controlled by biogeochemical processes rather than hydrological processes during the late water connection stage (Fig. 8c). A temporally variable control hypothesis of NO_3^--N export shifting from a flushing mechanism to a biogeochemical control mechanism has been proposed based on the hydrological connections on a seasonal scale (Ocampo et al. 2006a, b). Ocampo et al. (2006a) mentioned the role of denitrification in riparian zones and seems to support the conditions which were observed during this study. However, it should be emphasized that the denitrification potential was high in the upland soil (Table 2) and that the NO_3^--N leaching from the upland to the stream after the establishment of water connectivity helps explain the strongly reduced NO_3^--N concentrations in the upland soil during the late water connection stage.

The peak of NO_3^--N export following the discharge peak in E3 displayed the same trends as the Si concentrations in E3 and indicated a deep groundwater contribution. The NO_3^--N in the deep groundwater could have originated from the NO_3^--N rich snowmelt/rain water which recharged the deep groundwater via preferential flow paths (Creed et al. 1996; McHale et al. 2002). The soils in the Shibetsu watershed are characterized by having high rates of hydraulic conductivity. In addition, the AFW watershed is located in an area characterized by cold winters with a long snow-covered period. Thus, the soil freezing/thawing process during snowmelt season may produce more macropores and consequently enhance the N percolation into the deep groundwater (Jiang et al. 2012). Therefore, following a period of water connectivity, the NO_3^--N concentrations in the deep groundwater increased and then were exported to the stream which displayed high NO_3^--N concentrations later in the year.

Conclusions

This study was conducted to identify the water connectivity of an upland–riparian hillslope associated with stream NO_3^--N export in an agricultural and forested watershed. The groundwater tables at seasonal and rain event scales displayed the impacts of water connectivity from the upland, the interface, and the riparian forest to the stream. The water connectivity seemed to be established from the riparian forest to the stream during the

early water connection stage. The water connectivity from the upland to the stream seemed to have occurred during well and late water connection stages. A conceptualization was developed for the mechanisms of NO_3^--N export related to the hillslope water connectivity that was developed during rain events. The upland groundwater dominated the NO_3^--N export as a flushing mechanism, but was regulated by the hydrological connectivity of the upland–riparian zones, the antecedent soil moisture, and the groundwater table. The flushing of NO_3^--N in the riparian zones occurred during the early water connection stage. Then the NO_3^--N flushing to the upland area increased during the well water connection stage and was attributed to the high antecedent soil moisture or the high shallow groundwater table depth in the upland. Although the upland shallow groundwater was still the primary water source for the stream during rain events during the late water connection stage, the shallow groundwater was a limited NO_3^--N source because denitrification in the upland soil resulted in low NO_3^--N concentrations from the water source. Although the conceptual model was developed to help explain the N export through the concepts of water connectivity, the conceptual model should undergo additional testing and validation in the future with a larger number of rain events to make the conceptual model more robust due to the complex internal dynamics of shallow groundwater, NO_3^--N transport, and biogeochemical reactions.

References

Agricultural Department of Hokkaido Government (2002–2009) Standard fertilizer application for Hokkaido: Sapporo **(in Japanese)**

Anderson MG, Burt TP (1990) Subsurface runoff. In: Anderson MG, Burt TP (eds) Process studies in hillslope hydrology. Wiley, Chichester, pp 365–400

Burt TP, Pinay G (2005) Linking hydrology and biogeochemistry in complex landscapes. Prog Phys Geog 29(3):297–316

Creed IF, Band LE (1998a) Exporting functional similarity in the export of nitrite-N from forested catchments: a mechanistic modeling approach. Water Resour Res 34:3079–3093

Creed IF, Band LE (1998b) Export of nitrogen from catchments within a temperate forest: evidence for a unifying mechanism regulated by variable source area dynamics. Water Resour Res 11:3105–3120

Creed IF, Band LE, Foster NW, Morrison IK, Nicolson JA, Semkin RS, Jeffries DS (1996) Regulation of nitrite-N release from

temperate forest: a test of N flushing hypothesis. Water Resour Res 32:3337–3354

Gerritse RG, Adeney JA, Hosking J (1995) Nitrogen losses from a domestic septic tank system on the Darling Plateau in Western Australia. Water Res 29(9):2055–2058

Hayakawa A, Shimizu MK, Woli KP, Kuramochi K, Hatano R (2006) Evaluating stream water quality through land use analysis in two grassland catchments: impact of wetlands on stream nitrogen concentration. J Environ Qual 35:617–627

Hayakawa A, Nakata M, Jiang R, Kuramochi K, Hatano R (2012) Spatial variation of denitrification potential of grassland, windbreak forest, and riparian forest soils in an agricultural catchment in eastern Hokkaido, Japan. Ecol Eng 47:92–100

Hill AR (1996) Nitrate retention in stream riparian zones. J Environ Qual 25:743–755

Hill AR, Kemp WA, Buttle JM, Goodyear D (1999) Nitrogen chemistry of subsurface storm runoff on forested Canadian Shield hillslopes. Water Resour Res 35:811–821

Inamdar SP, Mitchell MJ (2006) Hydrologic and topographic controls on storm-event exports of dissolved organic carbon (DOC) and nitrate across catchment scales. Water Resour Res 42:W03421. doi:10.1029/2005WR004212

James AL, Roulet NT (2007) Investigating hydrologic connectivity and its association with threshold change in runoff response in a temperate forested watershed. Hydrol Process 21:3391–3408

Jiang R, Woli KP, Kuramochi K, Hayakawa A, Shimizu M, Hatano R (2010) Hydrological process controls on nitrogen export during storm events in an agricultural watershed. Soil Sci Plant Nutr 56:72–85

Jiang R, Woli KP, Kuramochi K, Hayakawa A, Shimizu M, Hatano R (2012) Coupled land use and topography controls on nitrate-nitrogen dynamics in three adjacent watersheds. Catena 97:1–11

Lexartza-Artzal, Wainwright J (2009) Hydrological connectivity: linking concepts with practical implications. Catena 79:146–152

McGlynn BL, McDonnell JJ, Brammer DD (2002) A review of the evolving perceptual model of hillslope flowpaths at the Maimai catchments, New Zealand. J Hydrol 257:1–26

McHale M, McDonnell JJ, Mitchell MJ, Cirmo CP (2002) A field based study of soil- and groundwater nitrate release in an Adirondack forested watershed. Water Resour Res 38(4):WR000102

McNamara JP, Kane DL, Hobbie JE, George WK (2008) Hydrologic and biogeochemical controls on the spatial and temporal patterns of nitrogen and phosphorus in the Kuparuk River, arctic Alaska. Hydrol Process 22:3294–3309

Ocampo CJ, Oldham CE, Sivapalan M, Turner JV (2006a) Hydrological versus biogeochemical controls on catchment nitrate export: a test of the flushing mechanism. Hydrol Process 20:4269–4286

Ocampo CJ, Sivapalan M, Oldham C (2006b) Hydrological connectivity of upland–riparian zones in agricultural catchments: implications for runoff generation and nitrate transport. J Hydrol 331:643–658

Ohrui K, Mitchell MJ (1998) Spatial patterns of soil nitrate in Japanese forested watersheds: importance of the near-stream zone as a source of nitrate in stream water. Hydrol Process 12:1433–1445

Schade JD, Welter JR, Marti E, Grimm NB (2005) Hydrologic exchange and N uptake by riparian vegetation in and arid-land stream. J N Am Benthol Soc 24(1):19–28

Shoji S, Nanzyo M, Dahlgren RA (1993) Volcanic ash soils—genesis, properties and utilization, developments in soil science. Elsevier, Amsterdam, pp 1–288

Tachibana H, Nasu Y (2003) Measurement of runoff. In: The Japan Society for Analytical Chemistry, Hokkaido Branch (ed) Water analysis. Kagaku Dojin, Kyoto, pp 362–370 **(in Japanese)**

Vidon PGF, Hill AR (2004) Landscape controls on the hydrology of stream riparian zones. J Hydrol 292:210–228

Western AW, Bloschl G, Grayson RB (2001) Toward capturing hydrologically significant connectivity in spatial patterns. Water Resour Res 37:83–97

Woli KP, Nagumo T, Kuramochi K, Hatano R (2004) Evaluating river water quality through land use analysis and N budget approaches in livestock farming areas. Sci Total Environ 329:61–74

Wood EF (1999) The role of lateral flow: over- or underrated. In: Tenhunen JD, Kabat P (eds) Integrating hydrology, ecosystem dynamics and biogeochemistry in complex landscapes. Wiley, Chichester, pp 197–215